BUCKLING ANALYSIS OF VARIABLE STIFFNESS PANELS MANUFACTURED BY FABRIC STEERING TECHNOLOGY

Z. Xiao[1], and P. Harrison[1]

[1]School of Engineering, University of Glasgow, Glasgow, G12 8QQ, UK
Zhaofei.xiao@glasgow.ac.uk; Philip.harrison@glasgow.ac.uk
Keywords: Variable Stiffness Panel, Fabric steering, Buckling, Strength prediction

ABSTRACT

This paper describes the development of a design tool, SteerFab, created for generation and analysis of variable stiffness panels. SteerFab generates the shape of both the un-steered and steered fabric via kinematic modelling [1]. Fibre angles and fabric thickness are then mapped into Abaqus Standard™ using bi-linear interpolation, prior to structural analysis. An automated genetic algorithm is developed to seamlessly connect the MatLab-based SteerFab code with the finite element analysis, in order to find the optimum steered pattern for a given structural geometry and loading condition. The final steered-fibre pattern is used to guide the fabric steering process developed at the University of Glasgow. The performance of various laminates, including straight-fibre, steered-fibre, and straight/steered hybrid laminates, are evaluated on two rectangular plates with and without a centre hole. An optimised steered-fibre pattern is predicted to achieve about a 9% improvement in buckling resistance, compared to the best straight fibre laminate [2, 3] of the same weight for a 300 mm × 400 mm plate. For the plate with a centre hole, the improvement in buckling increases to 14%. Similar enhancement is observed in AFP-manufactured variable stiffness panels [2].

1 INTRODUCTION

Fibre reinforced composites are commonly used in aerospace and automotive industries for lightweight design. The usage of composite materials in Boeing 787 and the life module (body structure) of BMW i3 has reached approximately 50 wt.% [4, 5]. Current advanced composite laminates are usually manufactured by stacking straight-fibre plies at certain fixed angles (e.g. 0°, 90°, ±45°). However, using a less-constrained approach, various researchers have aimed to increase the design space by continuously changing the fibre orientations across the laminate, leading to Variable Stiffness Panels (VSPs) and novel manufacturing processes have been developed to manufacture these panels.

Compared to straight-fibre laminates, the buckling resistance of VSP composites panels can be improved by over 10% [3, 6-8] and the failure load is also improved by as much as 25% [2]. Importantly, for a rectangular panel containing a centre hole, the curvilinear fibre path in VSPs means that failure initiates away from the hole, reducing the effect of the cut out on the panel's structural performance [2]. Researchers have begun to explore the applications of fibre steering in the aerospace industry, such as aeroplane fuselage panels and T-shaped stiffened skin panels [9, 10].

Fibre placement technologies, e.g. Automated Tape Laying (ATL) and Automated Fibre Placement (AFP), have been used in the aerospace industry to manufacture advanced composites structures [3, 11-13]. A typical fibre placement actuator head is shown in Figure 1. Previously, these technologies have usually been used to manufacture straight-fibre laminates. While wide carbon fibre tape is laid down in ATL, AFP deposits narrow fibre tows, which offers the possibility of tow steering [12, 13]. Indeed AFP has been specifically developed to deposit carbon fibres with continuously changing orientations. However, the VSPs made by AFP have three typical defects caused by in-plane bending deformation of the fibre tows [14-17] namely, (a) gaps between tows, (b) tow overlapping and (c) tow wrinkles (see Figure 2). Pre-impregnated tows are commonly used in AFP, but dry tows are drawing increasing attention for this application, as their low stiffness means they are easier to manipulate during tow deposition processes [1, 15, 16, 18]. Continuous Tow Shearing (CTS) technology developed by Kim et al. [15, 16] is a novel variant of conventional AFP, designed to reduce manufacturing defects. CTS uses

in-plane shear instead of bending to create curvilinear fibre paths eliminating both tow gaps and overlaps. Nevertheless, the fibre is still deposited tow by tow and layer by layer, which limits production rates. Furthermore, the complicated robot head of AFP makes the capital investment of fibre placement technologies very high. Hence, there is a need to both improve production rate and reduce manufacturing cost of VSPs. To this end, a novel low-cost fabric steering technology is proposed here. The technique is supported by a dedicated numerical design tool to assist the development and analysis of the low-cost manufacturing process. The remainder of this paper is organised as follows; Firstly, a novel design tool developed in this paper is introduced, and then the capability of the tool is demonstrated by an optimisation of buckling resistance for composites panels.

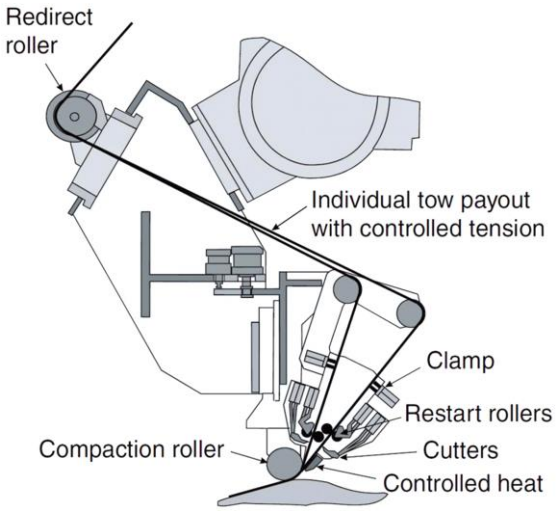

Figure 1. Typical robot heat for automated fibre placement [12]

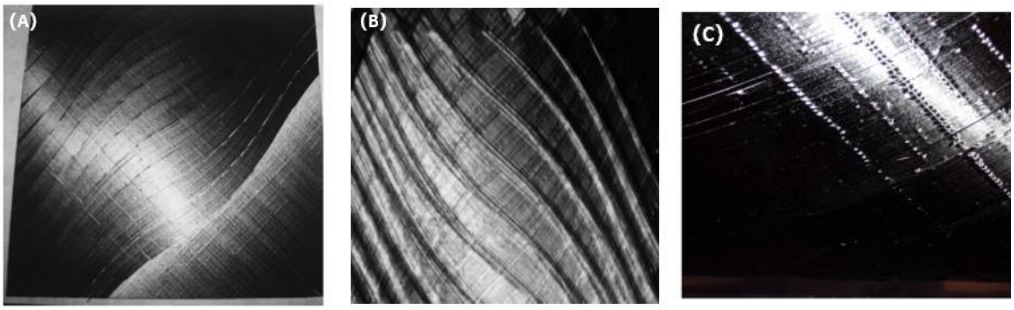

Figure 2. Common defects in VSPs manufactured by AFP: (A) tow gaps [3]; (B) tow overlapping [3]; (C) tow wrinkle [17]

2 DEVELOPMENT OF THE DESIGN TOOL (STEERFAB)

Novel low-cost fibre steering technology is currently under development at the University of Glasgow, details of the method will be reported in the near future. It will be shown that, through manipulating engineering fabrics, curvilinear fibre paths can be created to manufacture VSPs. In order to support manufacture and also to analyse the mechanical properties of VSPs, a design and analysis tool that can predict the steered-fibre pattern and transfer the fibre angle orientations into finite element analysis is required. In a previous study [1], a numerical code, VariFab, was developed to create a mesh with arbitrary perimeter shape and fibre angle variability. The VariFab code has been further developed in this work to create specific curvilinear fibre paths similar to those used in AFP-manufactured VSPs. The new code is named SteerFab.

The SteerFab code is designed as a comprehensive tool combining the functions of steered-fibre

pattern design, mechanical properties analysis and optimisation. The working process of SteerFab consists of four main steps, see Figure 3 (A) – (F).

Step 1: The mesh of initial undeformed blank (A) and the corresponding steered fabric pattern (B) are generated by a kinematic algorithm [1, 19].

Step 2: The element information (coordinates of elements and nodes) are extracted (D) from a finite element model created in Abaqus Standard™ (C).

Step 3: Fibre orientation and fabric thickness from the steered pattern are mapped into the finite element (FE) model using bi-linear interpolation (E).

Step 4: Mechanical properties of the steered pattern are investigated through the simulation in Abaqus (F). After the simulation, the SteerFab code extracts data from the Abaqus model for post-simulation analysis.

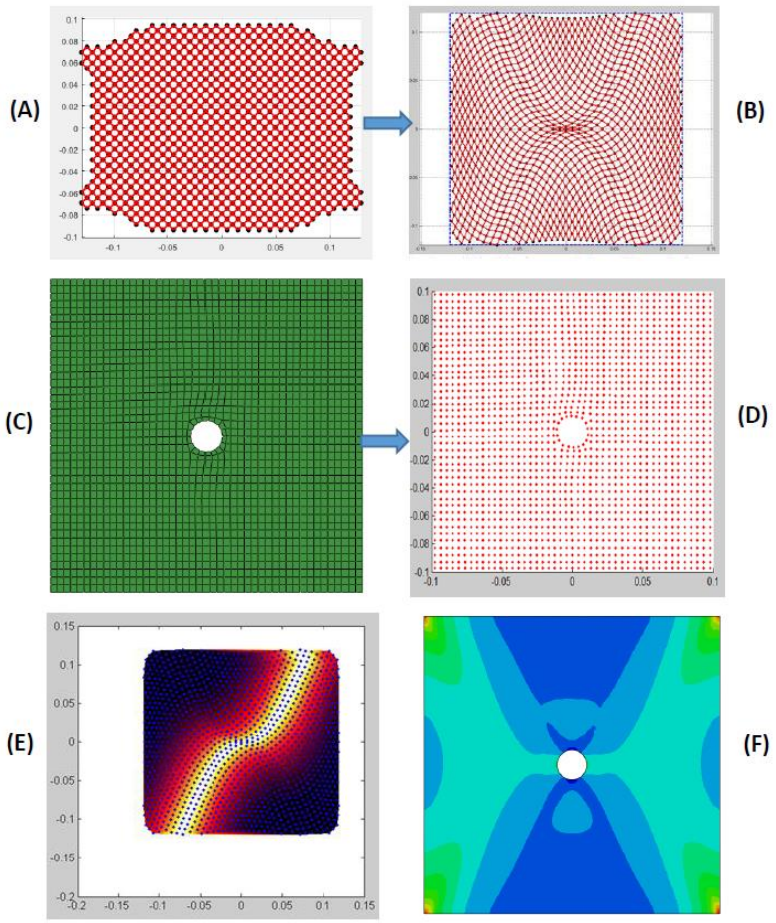

Figure 3 SteerFab code working process: (1) mesh generation of initial undeformed shape (A) and the steered fabric pattern (B); (2) Abaqus model element information extraction (C)-(D); (3) Fibre orientation and fabric thickness mapping (E); (4) FEA stress analysis in Abaqus (F)

Two main functions in the SteerFab code support the investigation of mechanical properties of the steered fabric laminates.

Steered pattern generation function

In the SteerFab code, a function, *a*, controls the shear angle of each element lying along the horizontal centre line, starting from the centre of the mesh and moving towards its boundary. There is no limit on the format of this function. For example, it can take the form of a high-order polynomial, a parabolic function or a trigonometric function. Figure 4 shows various steered-fibre patterns created by different control functions.

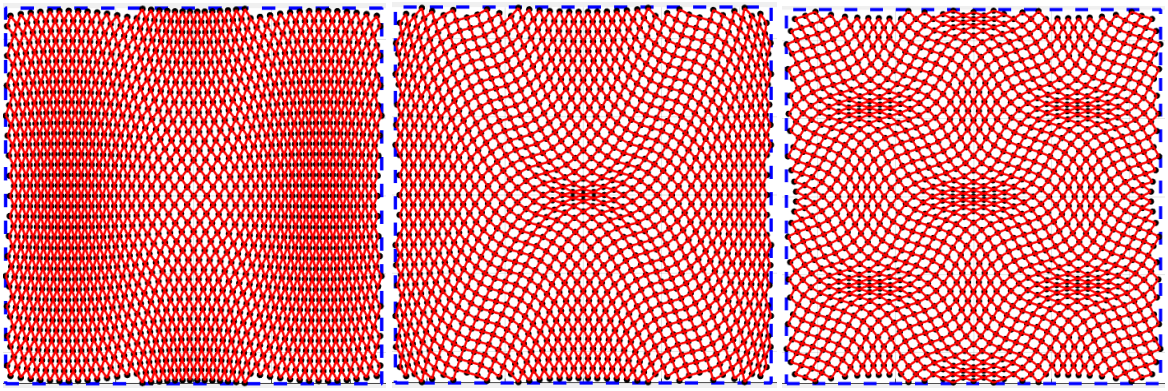

Figure 4 Various steered patterns created in SteerFab by different control functions

Straight/steered fabric hybridization function

In addition to creating and analysing a single steered-fibre pattern, the SteerFab code can also superimpose the information of different steered-fibre patterns into a single input file for stress analysis in Abaqus. Furthermore, unidirectional straight-fibre plies can be mixed with steered-fibre plies to create steered/straight fibre hybrid laminates, extending the design space even further. Figure 5 schematically shows both multiple steered fibre and combined steered and straight fibre hybrid laminates.

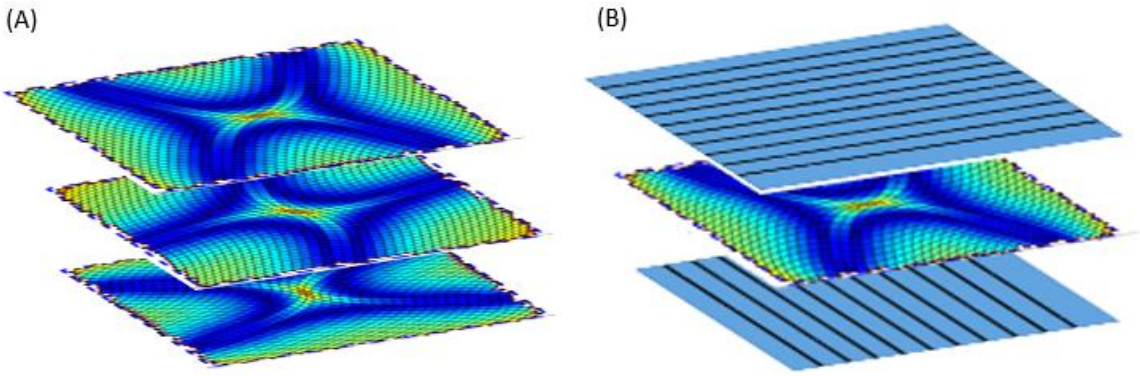

Figure 5 Schematics of steered/steered (A) and steered/straight (B) fibre laminates

3 PREDICTING THE BUCKLING BEHAVIOUR OF STEERED FIBRE LAMINATES

This section describes the details of the creation of steered fibre laminates using SteerFab, and the subsequent structural analysis of the laminates using Abaqus, focusing on buckling behaviour.

3.1 Steered fibre pattern creation

The steering pattern is controlled by the function, a. For the range of the parameter, t (the distance between a point on the horizontal axis to the centre of the steered pattern);

$$a = \mathrm{F}(\mathrm{FactorA}) \tag{1}$$

Variation of FactorA in Eq. (1) changes the profile of a, generating different steered patterns. The values of FactorA, investigated in the present work are: FactorA = [10; 25; 30; 35; 40; 45; 50; 52]

FactorA controls the maximum shear angle on the vertical edges of the steered fabric on the horizontal axis, as shown in Figure 6. A manufacturing constraint was set in SteerFab, namely, if the generated steered pattern includes shear angles exceeding 60°, the steered pattern is recognised as unrealistic and is not included in the evaluation. Hence, the upper limit of FactorA value range is 52.

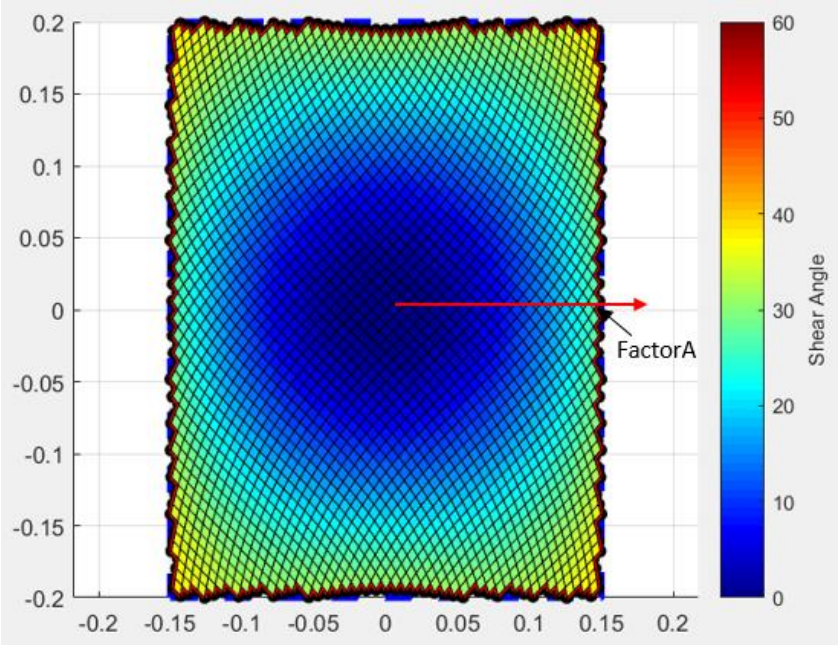

Figure 6 A steered pattern with the indication of max shear angle on the horizontal axis (FactorA)

Information from the generated steered patterns, such as tow angle and fabric thickness, are mapped to a finite element model for stress analysis. Regarding the fabric thickness, T, at this stage the fabrics are considered incompressible with a constant fibre volume fraction. Hence, the T is calculated by the function below:

$$T = T_0 / \cos\theta \tag{2}$$

where T_0 is the original thickness and θ is the shear angle.

3.2 Buckling simulation in Abaqus Standard™

Two FE models were created to investigate the performance of VSPs using rectangular plates with and without a centre hole. The geometries and corresponding meshes of these two types of plates are shown in Figure 7, both of them measure 300 mm × 400 mm. The diameter of the centre hole in Figure 7b is 90 mm, providing a D/W (diameter/width of the specimen) ratio of 0.3. Stiffness predictions are made using classical laminate theory. The boundary conditions are schematically shown in the Figure 7a. The bottom edge is fully clamped. The displacements and rotations of all the nodes on the top edge are fixed, apart from the displacement in the Y direction. The out-of-plane displacement on the two vertical edges is constrained (w=0). Each element on the top edge is applied a load of -1 N. The 'Perturbation – Buckle' step in Abaqus is used to conduct the buckling simulation. After the simulation, an eigenvalue for Mode 1 buckling is provided. The buckling load is equal to the eigenvalue multiplied by the element loading along the top edge.

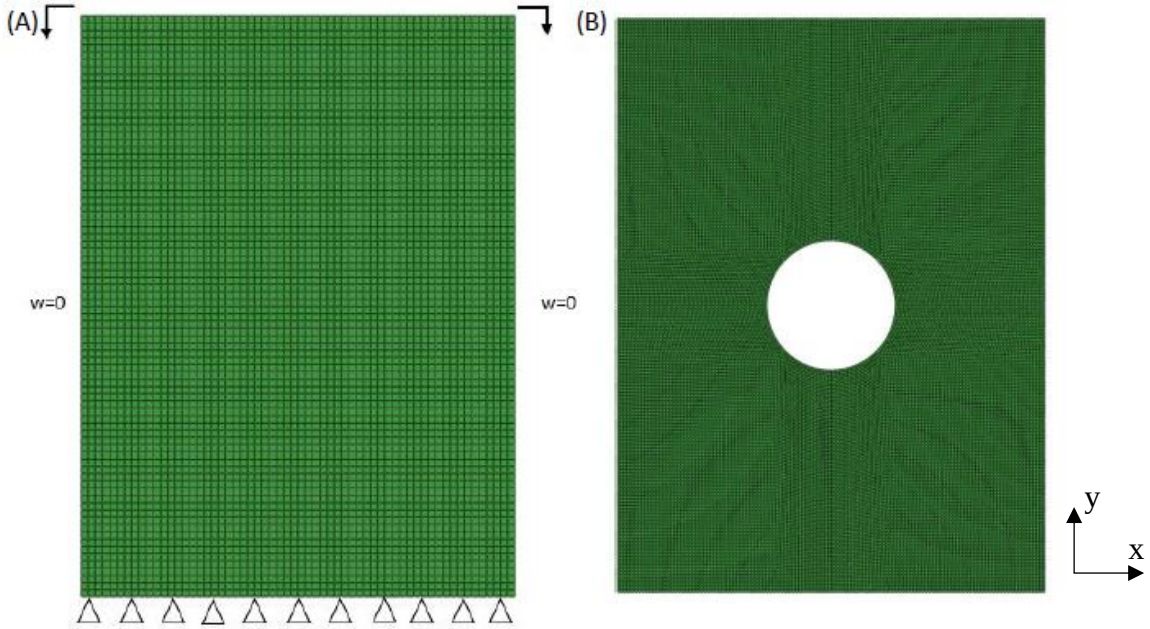

Figure 7 The mesh and geometry of the 300mm × 400mm panels (A) without a hole and (B) with a central hole (hole size dia. 90mm)

Individual ply properties are listed in Table 1. Eight laminate layups were analysed, including straight-fibre laminates, steered-fibre laminates, and hybrid straight/steered laminates, as listed in Table 2. This choice of layups is motivated by the work of Lopes et al [2, 7]. SteerFab was developed to allow the analysis of a combination of straight and steered fibre ply layups, creating hybrid straight/steered fibre laminates. SteerFab users can arbitrarily define the angle of the straight-fibre plies in the hybrid layup. In this way, pure steered laminates can be compared with both pure straight-fibre laminates (with arbitrary ply angles) and hybrid straight/steered fibre laminates.

Table 1 Properties of the carbon fibre composite materials.

Materials	AS4/9773 carbon fibre-epoxy system
Manufacturers	Carbon fibre: Hexcel. Resin: Cytec
Material properties*	E_{11}: 129.8 GPa E_{22}: 9.2 GPa ν_{12}: 0.36 G_{12}: 5.1 GPa X_t: 2070 MPa X_c: 1160 MPa Y_t: 29 MPa Y_c: 157.9 MPa S: 91 MPa

* E is Young's modulus; G is shear modulus; ν is Poisson's ratio; Xt and Xc are the tensile and compression strengths at fibre longitudinal direction; Yt and Yc are the tensile and compression strengths at fibre transverse direction; S is shear strength.

Table 2 Information of the laminates investigated in this paper

	Straight-fibre laminates	**VSP**	**Hybrid laminates**
Laminates type	$[(90/0)_4]s$ $[(\pm45)_4]s$ $[(\pm45)_2/(90/0)_2]s$ $[(90/0)_2/(\pm45)_2]s$ $[(\pm45)_2/(\pm30)/(\pm45)/(\pm15)]s$	$[(\pm VSP)_4]s$	$[(\pm VSP)_2/(90/0)_2]s$ $[(\pm45)_2/(\pm VSP)_2]s$
Ply thickness	0.1397 mm		

The mass of the carbon composite is the same in all laminates (straight and steered). Hence, the thickness of straight-fibre laminates is increased to compensate for the mass increase in the VSPs due to shearing. The thickness of straight-fibre laminates, T_{sl}, is calculated as

$$T_{sl} = T_0 \times N_p \times C \quad (3)$$

where T_0 is the thickness of unsheared ply, Np is number of plies and C is a compensation factor. The compensation factor = (area of the initial unsteered fabric) / (area of steered fabric). In this case the area of the steered fabric is 300 mm × 400 mm. Figure 8 shows an example of the initial unsteered and steered fabric generated by SteerFab. The area enclosed by the blue perimeter was calculated by the SteerFab code.

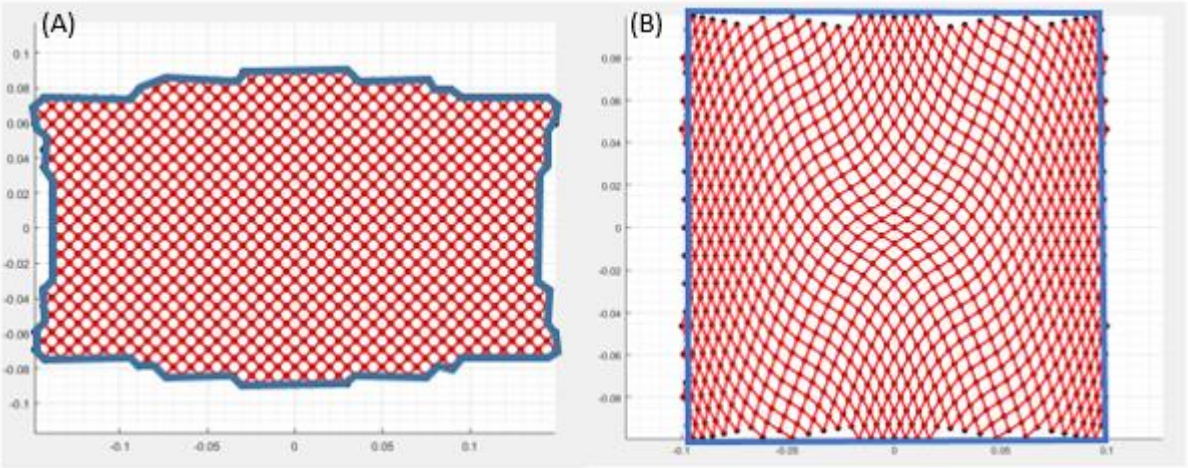

Figure 8 Initial unsheared shape (A); The corresponding steered pattern (B); The blue perimeter is used to calculate the area of the fabric before and after shear

4 RESULTS AND DISCUSSION

Figure 9 shows buckling loads of all the laminates listed in Table 2 for a 300 mm × 400 mm plate (Figure 7a) versus the maximum shear angle in the VSP. Note that the horizontal axis only applies to layups containing a steered fibre ply, hence all straight fibre layups have a constant buckling load when plotted against this parameter. All data in Figure 9 are normalised by the buckling load of the $[(\pm45)_4]$s laminate. Amongst the straight-fibre laminates, the $[(\pm45)_2/(90/0)_2]$s quasi-isotropic layup offers the best buckling resistance. Layup sequence also plays an important role, for example, the buckling load of the $[(\pm45)_2/(90/0)_2]$s quasi-isotropic layup (light blue line) is 10.2% higher than that of the $[(90/0)_2/(\pm45)_2]$s quasi-isotropic layup (dark orange line). In the former the (±45) plies are placed at the outer surface, providing an improved ability to resist the twisting deformations associated with buckling [8]. The $[(\pm45)_2/(\pm30)/(\pm45)/(\pm15)]$s layup (dark grey line), was identified to provide optimum buckling resistance in [2, 3, 7]. However, in this investigation this layup ranks only third among the straight-fibre laminates.

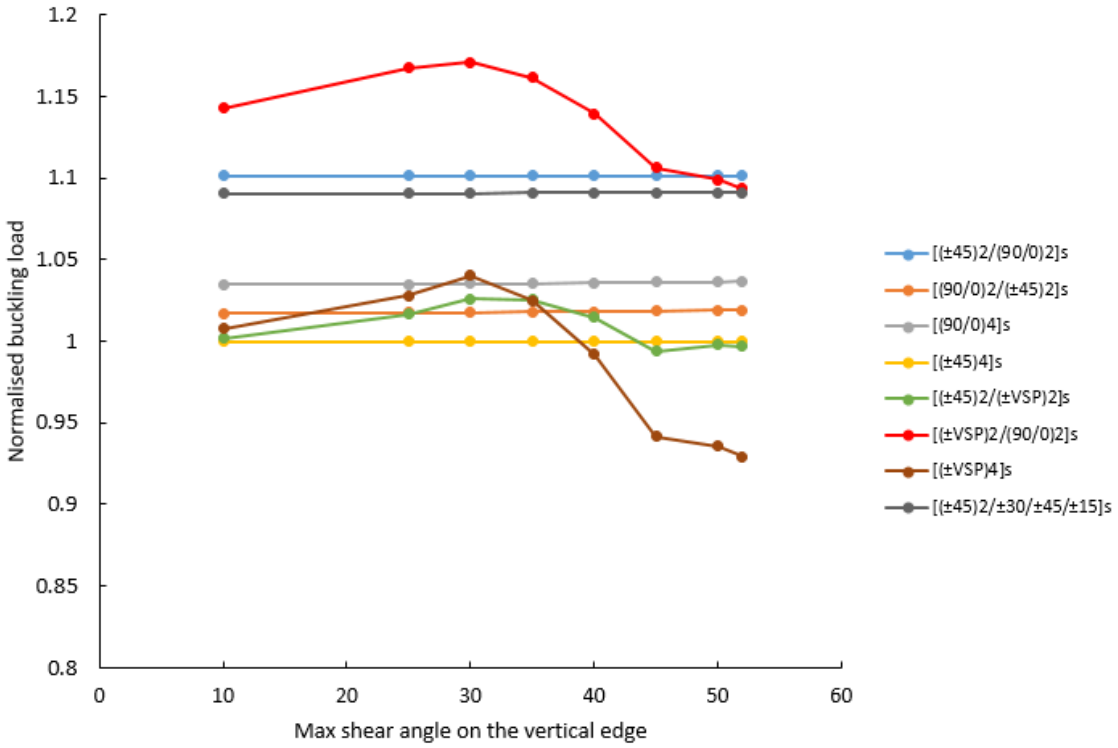

Figure 9 Normalised buckling load of all the laminates listed in Table 2 for a 300 mm × 400mm plate. Each data point was normalised to the buckling load of the $[(\pm 45)_4]_s$ laminate

Regarding the buckling load of the pure VSP laminate (brown line), when the max shear angle on the vertical edges along the horizontal axis reaches 30°, the buckling load achieves its highest value. Nevertheless, the VSP laminate does not show significant improvement in buckling compared with the other two double-angle laminates (e.g $[(90/0)_4]_s$ (light grey line) and $[(\pm 45)_4]_s$) (light orange line). However, when the VSP is mixed with straight-fibre plies to create hybrid straight/steered fibre laminates, the improvement in buckling load becomes apparent. When the VSP replaces the (±45) plies in the $[(\pm 45)_2/(90/0)_2]s$ layup (blue line), the buckling load of the hybrid laminate ($[(\pm VSP)_2/(90/0)_2]s$) (red line) is improved by 5.4%, and is also 9.3% better than the optimum layup ($[(\pm 45)_2/(\pm 30)/(\pm 45)/(\pm 15)]_s$) (dark grey line) in the previous studies [2, 3, 7].

Table 3 compares the buckling loads of all the laminates both with and without a centre hole. The presence of the centre hole in the plate decreases the buckling load of all straight-fibre laminates by, on average ~11%. However, the decrease in straight/steered hybrid laminates is much smaller, closer to just ~5%; about half the decrease of purely straight fibre laminates. Figure 10 demonstrates the positive influence of fibre steering on the buckling resistance of the laminates from another perspective. Here the normalised buckling load of all the laminates for plates both with and without a hole are plotted side-by-side. The buckling load of laminates without a hole are normalised by the buckling load of the $[(\pm 45)_4]_s$ laminate (blue bars). The buckling load of laminates with a central hole are normalised by the buckling load of the $[(\pm 45)_4]_s$ laminate containing a hole (orange bars). It can be seen that, for the plates with a centre hole, the improvement in buckling load of the straight/steered hybrid laminate ($[(\pm VSP)_2/(90/0)_2]s$) now becomes 7.2% compared to the conventional ($[(\pm 45)_2/(90/0)_2]s$) quasi-isotropic layup and 13.9% compared to the 'optimum' straight fibre laminate layup proposed by Lopes et al [2, 7]. In contrast, the VSP developed in [2] shows an improvement of ~10% in buckling load compared to the 'optimum' straight fibre laminate.

Table 3 Buckling loads of the investigated laminates

	Plate without hole	**Plate with dia. 90mm hole**	**Percentage reduction**
$[(90/0)_4]s$	20.10 kN	17.43 kN	13.3%
$[(\pm45)_4]s$	19.47 kN	17.52 kN	10%
$[(\pm45)_2/(90/0)_2]s$	21.79 kN	20.09 kN	7.8%
$[(90/0)_2/(\pm45)_2]s$	19.76 kN	17.31 kN	12.4%
$[(\pm45)_2/(\pm30)/(\pm45)/(\pm15)]s$	21.01 kN	18.91 kN	10%
$[(\pm VSP)_4]s$	19.61 kN	18.81 kN	4.1%
$[(\pm VSP)_2/(90/0)_2]s$	22.96 kN	21.54 kN	6.2%
$[(\pm45)_2/(\pm VSP)_2]s$	19.86 kN	18.74 kN	5.6%

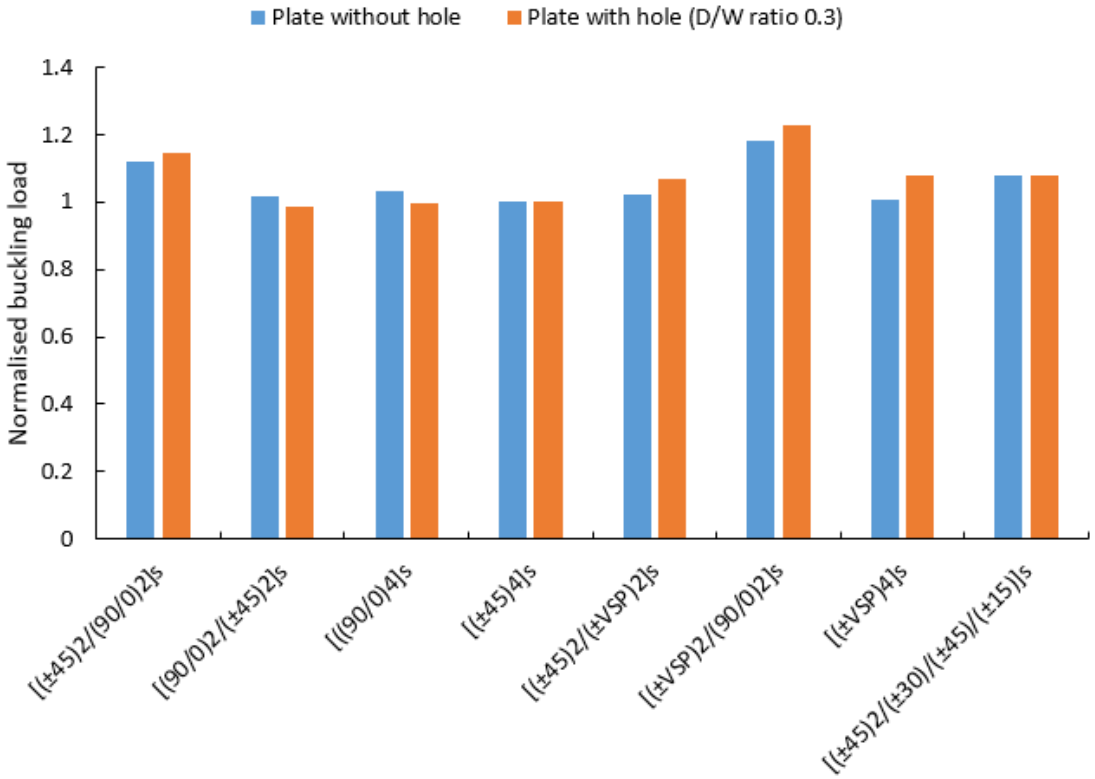

Figure 10 Normalised buckling load of the investigated laminates. All the data points were normalised to the buckling load of $[(\pm45)_4]s$

5 CONCLUSIONS

A comprehensive design and analysis tool, SteerFab, was developed to explore various steered patterns and investigate the mechanical properties of VSPs. It provides numerical support for the fabric steering technology developed at the University of Glasgow. The results demonstrate how when steered fabrics are mixed with (90°) and (0°) plies to create the hybrid laminates, e.g. $([(\pm VSP)_2/(90/0)_2]s)$, the buckling load becomes the highest among all the investigated laminates. The benefit brought by the VSP becomes even more significant in the case of a plate with a central hole. Compared to the conventional QI $([(\pm45)_2/(90/0)_2]s)$ and the 'optimum' layup $([(\pm45)_2/(\pm30)/(\pm45)/(\pm15)]_s)$ [2, 7] with a central hole, the buckling load of the hybrid laminate is improved by 7.2% and 13.9% respectively.

ACKNOWLEDGEMENTS

The authors would like to thank the Engineering and Physical Sciences Research Council (EPSRC) for funding support (EP/P021573/1) of this 2-D Forming of Low Cost Steered Fibre Laminates.

REFERENCES

1. Abdiwi, F., Harrison, P., Koyama, I., Yu, W.R., Long, A.C., Corriea, N., and Guo, Z., *Characterising and modelling variability of tow orientation in engineering fabrics and textile composites.* Composites Science and Technology, 2012. **72**(9): p. 1034-1041.
2. Lopes, C.S., Gurdal, Z., and Camanho, P.P., *Variable-stiffness composite panels: Buckling and first-ply failure improvements over straight-fibre laminates.* Computers and Structures, 2008. **86**: p. 897-907.
3. Tatting, B.F. and Gurdal, Z., *Design and Manufacture of Elastically Tailored Tow Placed Plates.* Tech. rep., NASA, 2002. **NASA/CR-2002-211919**.
4. Brosius, D. *Boeing 787 Update*. 2007 [cited 2018; Available from: https://www.compositesworld.com/articles/boeing-787-update.
5. Starke, J., *Carbon composites in automotive structural applications*, in *EuCIA: Composites and Sustainability*. 2016: Brussels.
6. Gürdal, Z., Tatting, B.F., and Wu, C.K., *Variable stiffness composite panels: Effects of stiffness variation on the in-plane and buckling response.* Composites Part A: Applied Science and Manufacturing, 2008. **39**(5): p. 911-922.
7. Lopes, C.S., Camanho, P.P., Gurdal, Z., and Tatting, B.F., *Progressive failure analysis of tow-placed, variable-stiffness composite panels.* International Journal of Solids and Structures, 2007. **44**: p. 8493-8561.
8. Weaver, P.M., Potter, K.D., Hazra, K., Saverymuthapulle, M.A.R., and Hawthorne, M.T., *Buckling of Variable Angle Tow Plates: from Concept to Experiment*, in *50th AIAA Structures, Structural Dynamics, and Materials Conference* 2009: California.
9. Alhajahmad, A., Abdalla, M.M., and Gürdal, Z., *Optimal Design of Tow-Placed Fuselage Panels for Maximum Strength with Buckling Considerations.* Journal of Aircraft, 2010. **47**(3): p. 775-782.
10. Coburn, B.H., Wu, Z., and Weaver, P.M., *Buckling analysis of stiffened variable angle tow panels.* Composite Structures, 2014. **111**: p. 259-270.
11. Kisch, R.A., *Automated fibre placement historical perspective*, in *SAMPE 2006 International Symposium*. 2006: Long Beach, CA.
12. Evans, D.O., *Fibre placement*, in *ASM handbook*, Miracle, D.B. and Donaldson, S.L., Editors. 2001, ASM International. p. 1135 - 1140.
13. Lukaszewicz, D.H.J.A., Ward, C., and Potter, K.D., *The engineering aspects of automated prepreg layup: History, present and future.* Composites Part B: Engineering, 2012. **43**(3): p. 997-1009.
14. Kim, B., Hazra, K., Weaver, P., and Potter, K. *Limitations of fibre placement techniques for variable angle tow composites and their process-induced defects*. in *18th ICCM*. 2011. Jeju, KR.
15. Kim, B.C., Potter, K., and Weaver, P.M., *Continuous tow shearing for manufacturing variable angle tow composites.* Composites Part A: Applied Science and Manufacturing, 2012. **43**(8): p. 1347-1356.
16. Kim, B.C., Weaver, P.M., and Potter, K., *Manufacturing characteristics of the continuous tow shearing method for manufacturing of variable angle tow composites.* Composites Part A: Applied Science and Manufacturing, 2014. **61**: p. 141-151.

17. Wu, K., Tatting, B., Smith, B., Stevens, R., Occhipinti, G., Swift, J., Achary, D., and Thornburgh, R., *Design and Manufacturing of Tow-Steered Composite Shells Using Fiber Placement*, in *50th AIAA/ASME/ASCE/AHS/ASC Structures, Structural Dynamics, and Materials Conference*. 2009, American Institute of Aeronautics and Astronautics.
18. Veldenz, L., Di Francesco, M., Giddings, P., Kim, B.C., and Potter, K., *Material selection for automated dry fiber placement using the analytical hierarchy process.* Advanced Manufacturing: Polymer & Composites Science, 2018. **4**(4): p. 83-96.
19. Long, A.C., Wiggers, J., and Harrison, P., *Modelling the Effects of Blank-Holder Pressure and Material Variability on Forming of Textile Preforms*, in *8th Int. ESAFORM Conf. on Materials Forming*. 2004: Cluj-Napoca, Romania.